Four-Junction Wafer-Bonded Concentrator Solar Cells

Frank Dimroth, Thomas N. D. Tibbits, Markus Niemeyer, Felix Predan, Paul Beutel, Christian Karcher, Eduard Oliva, Gerald Siefer, David Lackner, Peter Fuß-Kailuweit, Andreas W. Bett, Rainer Krause, Charlotte Drazek, Eric Guiot, Jocelyne Wasselin, Aurélie Tauzin, and Thomas Signamarcheix

***Abstract*—The highest solar cell conversion efficiencies are achieved with four-junction devices under concentrated sunlight illumination. Different cell architectures are under development, all targeting an ideal bandgap combination close to 1.9, 1.4, 1.0, and 0.7 eV. Wafer bonding is used in this work to combine materials with a significant lattice mismatch. Three cell architectures are presented using the same two top junctions of GaInP/GaAs but different infrared absorbers based on Germanium, GaSb, or GaInAs on InP. The modeled efficiency potential at 500 suns is in the range of 49–54% for all three devices, but the highest efficiency is expected for the InP-based cell. An efficiency of 46% at 508 suns was already measured by AIST in Japan for a GaInP/GaAs//GaInAsP/GaInAs solar cell and represents the highest independently confirmed efficiency today. Solar cells on Ge and GaSb are in the development phase at Fraunhofer ISE, and the first demonstration of functional devices is presented in this paper.**

***Index Terms*—Concentrator photovoltaics, high-efficiency, multijunction, photovoltaic cells.**

I. Introduction

FOUR-JUNCTION solar cells are under development as the next-generation product for high-concentration photovoltaics to replace today's triple-junction technology. Lattice-matched and metamorphic triple-junction cells on Ge reach efficiency values up to 42% [1], [2] and the best inverted metamorphic GaInP/GaAs/GaInAs solar cell up to 44.4% [3]–[5]. Further improvements in cell performance are expected by adding an additional p-n junction with optimum bandgap energy. From detailed balance calculations, it is known that a combination of 1.9, 1.4, 1.0, and 0.5 eV absorbers is ideal to convert the 500×AM1.5 direct sun spectrum [6], which is the typical spectrum for concentrator photovoltaic applications. In reality, this material combination is not easy to achieve, mainly because III–V compounds with large bandgap are predominantly found for small lattice constants, whereas low-bandgap absorbers tend to have larger lattice constants. Lattice-mismatched growth using two metamorphic GaInAs junctions and two lattice constant grading layers has turned out to be a suitable method to form four-junction solar cells [3], [7], as well as transfer printing [8]. Wafer bonding is an alternative approach and has been used to form multijunction solar cells combining InP- and GaAs-based compounds [9]–[13]. In this paper, we present the latest status of a four-junction solar cell development using an upper GaAs-based GaInP/GaAs cell structure bonded to a lower GaInAsP/GaInAs cell structure on InP as schematically presented in Fig. 1(a). This cell includes only lattice-matched epitaxial growth, which results in the lowest threading dislocation densities. Two alternative cell architectures are introduced using a combination of wafer bonding and metamorphic growth to reach the optimum set of bandgap energies. Fig. 1(b) shows a cell on Germanium with a metamorphic GaInAs subcell bonded to a top GaInP/GaAs tandem. Fig. 1(c) shows a cell on GaSb bonded to an inverted metamorphic GaInP/GaAs/GaInAs triple-junction cell. All three designs use similar top cell absorbers, but the materials for the lower two subcells are different.

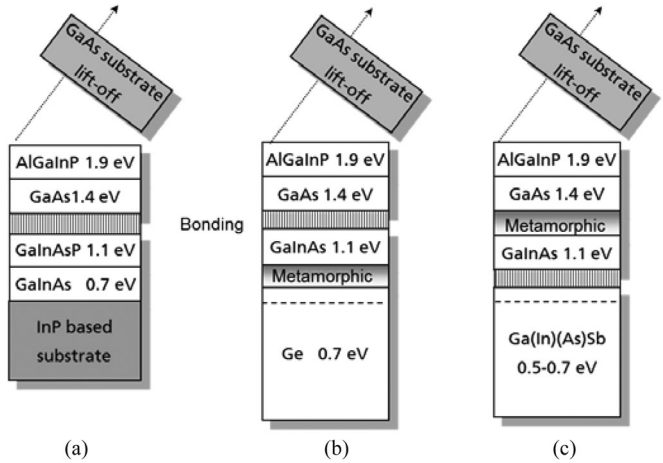

Fig. 1. Absorber and substrate materials for three wafer-bonded four-junction solar cells. (a) InP-based, (b) Ge-based, and (c) GaSb-based.

The cell structure on Germanium benefits from the lowest substrate cost and an established cell processing in the concentrator photovoltaic industry. GaSb, on the other hand,

Manuscript received June 16, 2015; accepted September 10, 2015. Date of publication December 1, 2015; date of current version December 18, 2015. This work was supported by the French Environment and Energy Management Agency (ADEME) through the "Investissement d'Avenir" program GUEPARD. The work at Fraunhofer ISE was supported in part by the German Ministry for Economics and Energy BMWi through the contract HekMod4 (0325750) and the European Union through the project CPVMatch (640873). The work of M. Niemeyer and F. Predan was supported through Ph.D. funding by the German Federal Environmental Foundation (DBU).

F. Dimroth, T. N. D. Tibbits, M. Niemeyer, F. Predan, P. Beutel, C. Karcher, E. Oliva, G. Siefer, D. Lackner, P. Fuß-Kailuweit, and A. W. Bett are with the Fraunhofer Institute for Solar Energy Systems ISE, 79110 Freiburg, Germany (e-mail: frank.dimroth@ise.fraunhofer.de; thomas.tibbits@ise.fraunhofer.de; Markus.Niemeyer@ise.fraunhofer.de; Felix.Predan@ise.fraunhofer.de; Paul.Beutel@ise.fraunhofer.de; christian.karcher@ise.fraunhofer.de; eduard.oliva@ise.fraunhofer.de; gerald.siefer@ise.fraunhofer.de; david.lackner@ise.fraunhofer.de; p.fuss-kailuweit@wavelabs.de; andreas.bett@ise.fraunhofer.de).

R. Krause, C. Drazek, E. Guiot, and J. Wasselin are with SOITEC S.A., 38190 Bernin, France (e-mail: Rainer.Krause@soitec.com; Charlott.Drazek@soitec.com; Eric.Guiot@soitec.com; jocelyne.wasselin@wanadoo.fr).

A. Tauzin and T. Signamarcheix are with CEA-LETI, 38054 Grenoble, France (e-mail: aurelie.tauzin@cea.fr; thomas.signamarcheix@cea.fr).

Color versions of one or more of the figures in this paper are available online at http://ieeexplore.ieee.org.

Digital Object Identifier 10.1109/JPHOTOV.2015.2501729

allows us to extend the spectral absorption range toward 0.5 eV (2480 nm) by using lattice-matched GaInAsSb compounds [14], [15]. Therefore, this is the only cell concept that reaches the optimum set of bandgap energies for a four-junction cell from detailed balance calculations [6], [16]. However, in reality, the performance of a specific multijunction solar cell stack is not only related to the bandgap energies of the materials but rather influenced by specific material properties such as absorption coefficient, mobility, minority carrier lifetime, and availability of suitable barrier materials. This paper, therefore, starts with a more detailed evaluation of realistic efficiency potentials for the wafer-bonded four-junction solar cells and then discusses experimental fabrication and recent results for each of the cell architectures.

A. Theoretical Modeling

Theoretical calculation were performed using a self-built code for calculating the absorption in each layer of a four-junction cell, using the transfer matrix method [17]. It was assumed that light is coherent throughout the whole device structure. To achieve a proper optical termination, the substrate was defined to have an infinite thickness. Absorption coefficients for the materials were taken from [18]–[22], as well as from in-house measurements at Fraunhofer ISE. For unknown compositions, the data were interpolated from the nearest available neighbors. A morphing algorithm was used for the interpolation of $n(\lambda)$ and $k(\lambda)$ data, which takes into account critical energy points where the slope of the dielectric functions changes significantly. Linear interpolation with composition was performed between these critical energy endpoints. The interpolation method was tested for Al_xGa_{1-x} As compounds and found to lead to excellent agreement with experimental results. The dielectric function of ternary and quaternary III–V compounds was then determined by using this morphing algorithm, and the transfer matrix method was used to calculate the expected absorption in each solar cell layer. The current of a subcell is then calculated for the AM1.5d spectrum by assuming that each absorbed photon creates one electron–hole pair, which contributes to the photocurrent.

The algorithm for the optimization of the four-junction solar cell followed a sequence of

1) finding the optimum bandgap combination by maximizing a fitness function defined as the sum of all bandgap energies multiplied by the photocurrent of the current limiting subcell; this represents an approximation to the power of the device;
2) applying a single-diode model to each junction to determine the overall dark-current characteristics of the four-junction cell;
3) optimizing P_{MPP} by assuming $J(V) =$ smallest photocurrent of all subcells minus the sum of the dark currents of the subcells.

Typical values have been assumed for the series resistance (15 mΩ·cm^{-2}) and grid shading (4%). These values are realistic and may be even improved in the future. The parallel resistance was taken as infinite. The reverse saturation current J_{rs} is a function of the bandgap energy of the material and may be determined from a thermodynamic limit approximation (Shockley–Queisser), or following the method described by Wanlass *et al.* [23], [24]. We used measured values of the best single-junction solar cells with similar material composition and adapted the values for J_{rs} for the exact bandgap energy by using the method of Wanlass with $J_{\mathrm{rs},i} = \beta T^3 e^{\frac{-E_g}{kT}}$, $\beta = Ae^{BE_g}[\mathrm{A}\cdot\mathrm{m}^{-2}\cdot\mathrm{K}^{-3}]$ and $A = 0.702548$; $B = 2.38585$. The saturation currents for the different subcells are listed in Table I. The different values reflect material-related differences between the compounds, and this is especially important for the performance of the indirect Ge junction, which shows a higher dark saturation current compared to direct III–V compounds in the same bandgap range.

TABLE I
REVERSE SATURATION CURRENTS J_{rs} DETERMINED FROM CURRENT–VOLTAGE CHARACTERISTICS OF SINGLE-JUNCTION SOLAR CELLS AND USED IN THE THEORETICAL MODEL

Material System	Saturation Current J_{rs}
AlGaInP (1.92 eV)	5.5×10^{-25} A/m^2
GaAs (1.42 eV)	1.6×10^{-16} A/m^2
GaInAs (1.08 eV)	2.0×10^{-10} A/m^2
GaInAsP (1.08 eV)	1.9×10^{-11} A/m^2
GaSb (0.73 eV)	6.7×10^{-05} A/m^2
GaInAs (0.71 eV)	2.1×10^{-04} A/m^2
Ge (0.67 eV)	3.1×10^{-03} A/m^2

TABLE II
MODELED *I–V* PARAMETERS FOR THE OPTIMIZED FOUR-JUNCTION CELL CONCEPTS UNDER 500×AM1.5D CONDITIONS

Device Concept	η [%]	V_{oc} [V]	J_{sc}/C [mA/cm^2]	FF [%]
InP-based cell (a)	53.8	4.376	14.2	86.7
Ge-based cell (b)	49.5	4.170	13.8	86.2
GaSb-based cell (c)	51.5	4.412	13.4	86.9

For calculating an optimum configuration for each four-junction solar cell, not only the absorber layers must be defined. MgF_2/Ta_2O_5 with a thickness of 127 and 75 nm deposited on a 30-nm AlInP window layer was assumed as the antireflective coating for all solar cells. The window layer was calculated to contribute partly to the photocurrent of the AlGaInP top junction as found from experimental results [25]. The influence of these upmost layers was verified by comparing the modeled absorption of the GaInP top cell to measured external quantum efficiencies. A good agreement was obtained for high-quality solar cells. Tunnel diodes, barrier layers, and bond layers were not included in the optimization as it may be assumed that such layers can be chosen from high-bandgap alloys, leading to negligible absorption loss.

The results of the theoretical model for all three four-junction solar cell designs of Fig. 1 are summarized in Table II. The calculations were performed for 500×AM1.5d (1000 W/m^2) conditions. The thickness of each subcell in the optimized four-junction device is chosen to ensure current matching between all junctions, but the thickness of the bottom cell was restricted to: 75 μm for Ge, 2.5 μm for GaInAs, and 5 μm for GaSb. We assumed that these are typical active layer thicknesses, which may

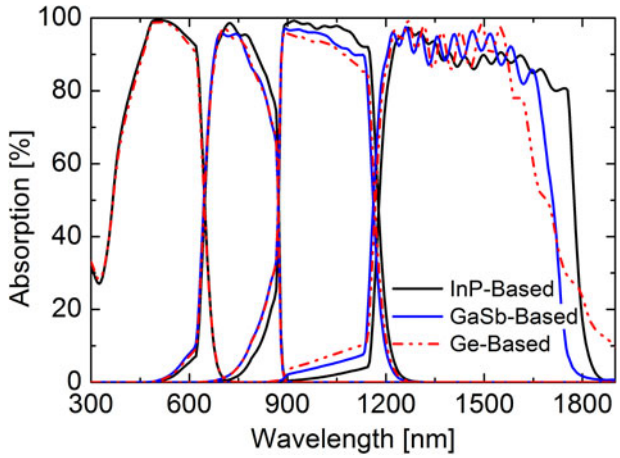

Fig. 2. Calculated absorption for the optimized four-junction solar cells in Fig. 1 using the transfer matrix method. The topmost layers were 127-nm MgF_2, 75-nm Ta_2O_5, and 30-nm AlInP. The thickness of the lowest absorber was restricted to 75-μm Ge, 2.5-μm GaInAs, and 5-μm GaSb. All other subcell thicknesses were chosen to reach current matching under AM1.5d conditions.

contribute to the photocurrent. From these calculations, we find that the InP-based GaInP/GaAs//GaInAsP/GaInAs cell structure has the highest potential and may reach efficiencies up to 53.8%, followed by the antimonide-based GaInP/GaAs/GaInAs//GaSb cell with a maximum efficiency of 51.5% and the Ge-based GaInP/GaAs//GaInAs/Ge cell with 49.5%. The absorption of each of these solar cell devices is plotted in Fig. 2. The most pronounced differences are observed in the wavelength range of the lowest junction. Germanium (0.67 eV) is an indirect semiconductor, and the absorption, therefore, has a long tail between 1600 and 1900 nm. GaSb (0.73 eV) and GaInAs (0.71 eV) are direct semiconductors, and the absorption is abrupt close to the bandgap. The absorption of GaInAs is extended 62 nm into the infrared compared with GaSb. It will be seen later that such a large difference is not necessarily found experimentally but obviously depends on the exact composition and lattice matching of the ternary GaInAs cell to the InP substrate.

The second subcell with a bandgap of 1.08 eV was adjusted in thickness to match the current of the bottom subcell, and consequently, the thicknesses of the GaAs cell with 1.42 eV and the AlGaInP cell with 1.92 eV were chosen accordingly to balance the photocurrents of all junctions. The differences in the absorption of the lowest subcell control the overall J_{sc} of the cell and the current consequently increases from the indirect Ge-based cell to the GaSb-based cell and to the InP-based cell. The voltage and fill factor (FF) on the other hand are strongly influenced by the dark saturation current, and again Ge has a significantly lower V_{oc} because of the high dark current, whereas the GaSb cell benefits both from low dark current and high bandgap of the bottom cell.

The theoretical model may be extended in the future to model also four-junction devices using a GaInAsSb bottom cell between 0.5 and 0.73 eV, which may allow even higher efficiencies. However, material constraints may lead to a higher dark saturation current, which has been shown to be of major importance for reaching the highest performance levels. In summary, assuming materials with sufficient diffusion length, the modeling results suggest that four-junction solar cell with >50% efficiency at 500 suns are, in fact, possible.

II. Experimental Details

All four-junction solar cells in Fig. 1 were realized experimentally. The III–V compound semiconductor layer structures were grown at Fraunhofer ISE by metal–organic vapor phase epitaxy using an AIX2800-G4 reactor (8 × 100 mm substrate configuration) for arsenides and phosphides and a CRIUS closed coupled showerhead reactor (7 × 100 mm configuration) for gallium antimonide. The substrates for InP, GaAs, and Ge had a diameter of 100 mm, whereas GaSb was grown on 2-in wafers placed in the middle of a 100-mm recess. Some of the InP-based solar cells were realized on InP-on-GaAs engineered substrates with a diameter of also 100 mm. These special wafers are a product of SOITEC and enabled by transfer of a thin (<1 μm) InP layer from a bulk substrate to a GaAs wafer using SmartCut technology [26].

Typical growth temperatures were between 530 and 700 °C, V/III ratios between 1 and 40. Arsine, phosphine and trimethylantimony were used as group-V precursors and trimethylgallium, trimethylindium, trimethylaluminium as group-III precursors. Further details are published in [9], [12], and [27]. All top tandem cell structures were grown in an inverted manner on a GaAs substrate, whereas all bottom cell structures were grown upright on Ge, InP, InP-on-GaAs, or GaSb.

All solar cell wafers were polished after the epitaxial growth to obtain a low surface roughness of <1 nm. Wafer bonding for InP-based solar cells was performed at SOITEC, using a proprietary process developed with CEA-LETI. All other wafers were bonded at Fraunhofer ISE using a single-wafer Ayumi SAB100 high vacuum tool, offering the possibility to remove surface oxides by a fast atom beam of Argon before joining the wafers at a bond force of 10 kN. This allowed high bond stability and low bond resistance in the range of 1–5 mΩ·cm^2. The bond interface for the InP-based cell (a) was formed between InP and GaAs, for the Ge-based cell (b) between GaAs and $Ga_{0.33}In_{0.67}P$ and for the GaSb-based cell (c) between GaSb and $Ga_{0.23}In_{0.77}P$.

The GaAs substrate on the top tandem cell was removed by chemical etching, and concentrator solar cell devices were processed using standard metal contacts and dielectric coatings. 75-nm Ta_2O_5 and 127-nm MgF_2 were evaporated onto the AlInP window layer as the antireflective coating. Solar cell devices had an area of typically 5.3 mm^2 with etched trenches of at least 10-μm depth separating the p-n junctions. Electrical characterization was carried out in the Fraunhofer ISE CalLab using a grating monochromator setup for the quantum efficiency [28], [29]; a multisource solar simulator [30] for 1-sun *I–V* characteristics; and a flash simulator for measurements under concentration. Both single-flash simulators, as well as a four-flash simulator (QuadFlash) with spectrum control, have recently been used [31], [32].

III. Results and Discussion

The following section summarizes characterization results for three different four-junction solar cell devices (according to

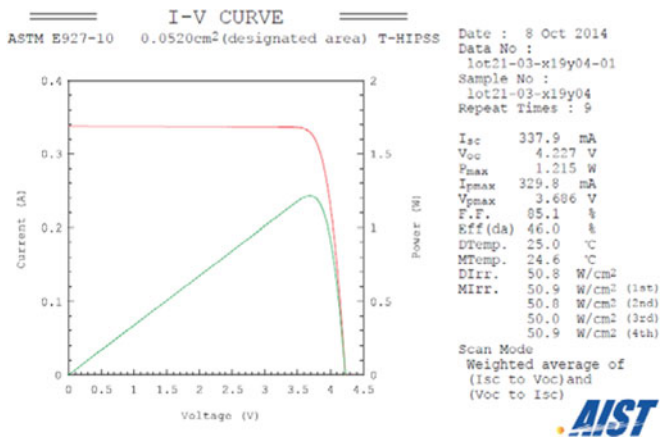

Fig. 3. *I–V* characteristics of a wafer-bonded GaInP/GaAs//GaInAsP/GaInAs four-junction cell measured at AIST/Japan under 508-fold concentration of the AM1.5d spectrum.

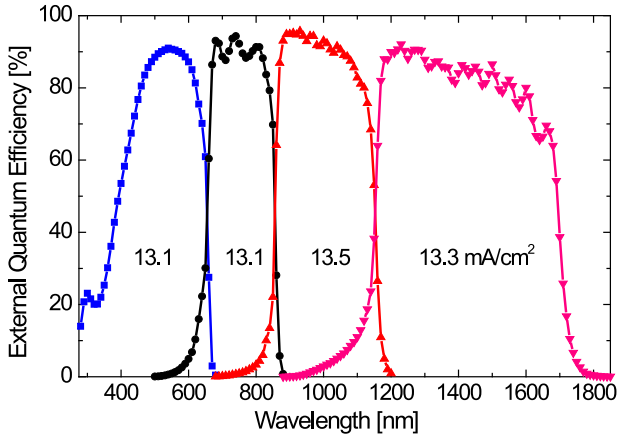

Fig. 4. External quantum efficiency of a GaInP/GaAs// GaInAsP/GaInAs four-junction solar cell grown on InP-on-GaAs engineered substrate. Numbers represent the calculated current densities for each junction under the AM1.5d ASTMG173-3 spectrum at 1000 W/m^2.

Fig. 1) using wafer bonding to join compounds with significant difference in lattice constant.

A. Four-Junction Solar Cell on InP

A more detailed discussion of the wafer-bonded GaInP/GaAs//GaInAsP/GaInAs four-junction solar cell was already published previously in [9], [10], [12], and [13] with a calibrated efficiency of 44.7% measured under 297×AM1.5d conditions. These devices were further developed in the meantime following an engineering approach and resulting in improved characteristics in respect to

1) current balance between subcells;
2) series resistance of emitter;
3) shading of metal contacts;
4) current collection and voltage of the GaInP top cell;
5) edge definition by steep mesa etch.

The best solar cell was sent for external validation to the Japanese Calibration Laboratory AIST. *I–V* characteristics were measured under the AM1.5d spectrum at 508-fold concentration, and an efficiency of 46.0% was confirmed for this concentrator cell with an area of 5.2 mm^2 (see Fig. 3). It should be mentioned that the cell was measured under spectrally matched conditions of a T-HIPPS solar simulator, leading to nearly identical irradiation conditions of 50.9, 50.8, 50.0, and 50.9 W/cm^2 for the first, second, third, and fourth subcell from the top, respectively. The same cell had been measured before at Fraunhofer ISE CalLab, obtaining an efficiency of 46.5% with a single-flash simulator leading to a surplus in current generation of 30% in the GaInAsP cell compared with AM1.5d conditions. It is known that this spectral mismatch of this simulator spectrum may lead to an overestimation of the FF, as discussed in [31], which was accounted for by a higher error bar. It is important for a proper calibration of multijunction solar cells to keep the spectral mismatch for each subcell under the simulator spectrum small.

Fig. 4 shows an external quantum efficiency of a solar cell, which was grown on InP-on-GaAs engineered substrate [26]. The use of an engineered substrate reduces manufacturing costs

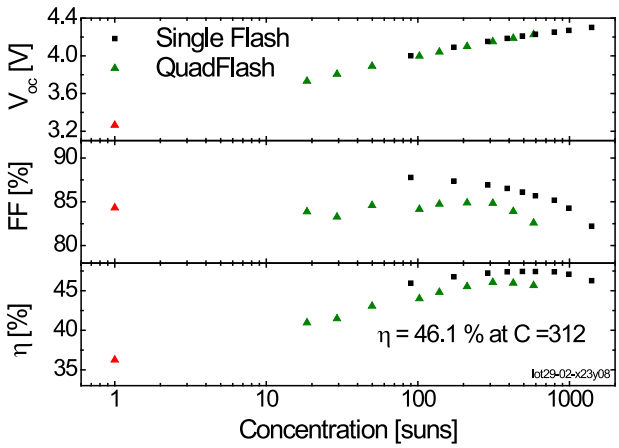

Fig. 5. *I–V* parameters of a wafer-bonded GaInP/GaAs// GaInAsP/GaInAs four-junction solar cell on InP-on-GaAs engineered substrate at different concentration levels, measured at Fraunhofer ISE CalLab under a single flash and the QuadFlash simulator. Additionally, the *I–V* parameters of the 1-sun measurement from the multisource simulator is shown. The QuadFlash allows us to match individually the spectrum incident on each subcell to the respective current generation under the AM1.5d ASTM G173-03 spectrum. A peak efficiency of 46.1% at 312-sun concentration was obtained for the QuadFlash simulator, compared with 47.4% at 389 suns with the single flash.

by replacing a 500-μm-thick InP bulk crystal by a $<$1-μm-thin seed layer transferred to GaAs. The cell is processed identical to a solar cell on an InP bulk wafer. The external quantum efficiency of all junctions reaches above 90%, and the subcell currents are matched within $\pm$2%. *I–V* characteristics have been plotted as a function of concentration in Fig. 5 for two measurements: one under a single-source flash simulator, resulting in a higher spectral mismatch, and one under a QuadFlash simulator with precise spectrum control. While an efficiency of 47.4% is measured under the single flash, the measurement shows an efficiency of 46.1% at 312-sun concentration using the QuadFlash simulator. The influence of the spectrum is seen in the FF, which is significantly increased under the single flash due to a higher current mismatch between the junctions. The QuadFlash result of $\eta = 46.1\%$ presents a new record for any solar cell

device and proves the outstanding material quality, which has been obtained for these devices.

B. Four-Junction Solar Cell on Ge

Four-junction solar cells were also realized by a combination of an inverted GaInP/AlGaAs top tandem solar cell with an upright metamorphic grown GaInAs/Ge bottom tandem cell. Both solar cell structures were joined by surface activated direct wafer bonding at Fraunhofer ISE. The diffusion of the lowest Ge junction was performed in the epitaxy reactor followed by the growth of a Ga_{1-x} In_xAs metamorphic buffer, a tunnel diode, and the $Ga_{0.82}In_{0.18}As$ subcell. After bonding the tandem cells together, the GaAs substrate was removed and the solar cells processed. The material quality of the $Ga_{0.82}In_{0.18}As$ cell depends strongly on the threading dislocation density, which can be achieved on top of the metamorphic buffer. This has been measured by cathodoluminescence to be less than 10^6 cm^{-2}. At this low level of dislocation density, no significant effect on the device characteristics is expected. Quantum efficiencies and *I–V* characteristics versus concentration are shown in Fig. 6. The photogenerated current densities in each subcell are approximately 1 mA/cm^2 lower compared with the InP-based structure. In addition, the device efficiency peaks already at 188-sun concentration due to a high resistance originating from the lower tunnel diode or the bond interface. Further optimization of the cell structure will improve the efficiency in the future.

C. Four-Junction Solar Cell on GaSb

Finally, first experimental results are presented for an antimonide based four-junction solar cell device. An inverted metamorphic GaInP/GaAs/GaInAs structure with Ga_{1-x} In_xP lattice grading between the GaAs and $Ga_{0.76}In_{0.24}As$ subcell was realized and bonded to a simple n-on-p GaSb cell. The latter one was formed by epitaxy growth of a Te-doped emitter layer on a Si-doped base. This cell structure did not yet include any passivation layers on the front or back side of the device. The wafers were joined using the surface activated bonding at Fraunhofer ISE and low bond resistances <5 m$\Omega\cdot$cm^2 were confirmed with test samples.

The external quantum efficiency in Fig. 7 shows good performance for the upper three subcells, whereas the lowest GaSb junction still suffers from significant recombination losses. These losses are explained by the missing front surface passivation layer of the GaSb cell. Carriers that are diffusing to the front surface of the GaSb cell are likely to recombine in the vicinity of the bond interface, which is formed between n-GaInP and the n-GaSb emitter. The region around the bond interface is characterized by a high defect density, which originates from the surface activation with Argon atoms prior to the bonding. It was found for GaAs and Si that the fast atom beam treatment results in an amorphous layer with a thickness between 2 and 5 nm [33]–[35], which is likely to suffer from high nonradiative recombination. Further improvement of the GaSb-based cell design requires the introduction of a transparent front surface passivation layer to prevent minority carriers from reaching the bond interface. Overall, the cell structure reaches already

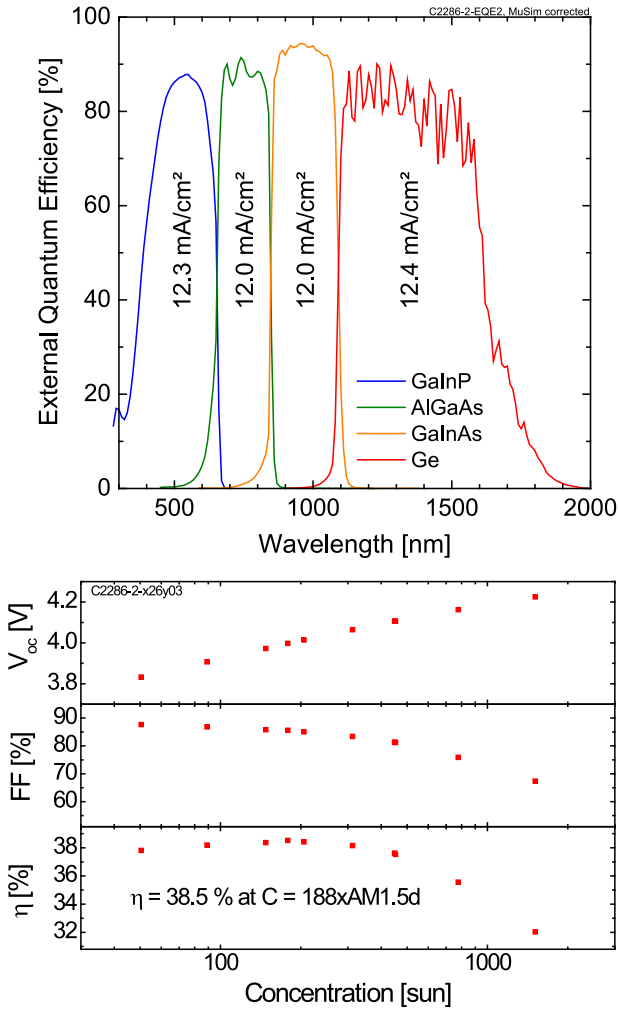

Fig. 6. External quantum efficiency of a GaInP/AlGaAs//GaInAs/Ge four-junction solar cell with calculated current densities for each junction under the AM1.5d ASTMG173-3 spectrum at 1000 W/m^2 (top) and *I–V* parameters versus concentration using a single flash solar simulator (bottom). The efficiency of 38.5% has, therefore, a higher uncertainty of 7% relative.

open-circuit voltages up to 3.9 V under concentration and an efficiency of approximately 29.1% at 194 suns.

IV. Summary and Conclusion

Multijunction solar cells with four or more junctions will be necessary to reach conversion efficiencies above 50% under concentrated sunlight in the future. Detailed balance calculations suggest that 65% efficiency is obtainable at 500× concentration using a combination of absorbers with 1.9, 1.4, 1.0, and 0.5 eV. In reality, optical losses by front surface reflection, parasitic absorption in barrier layers, grid shading and electric losses by recombination and various resistances will keep real efficiencies well below this number. We have developed a more realistic model starting from measured material data and calculating absorption by the transfer matrix method. Current–voltage characteristics are obtained from a simple single-diode model for each junction. Three architectures for four-junction devices based on InP, Ge, and GaSb were discussed, and the model predicts that efficiencies up to 53.8% are achievable. Of

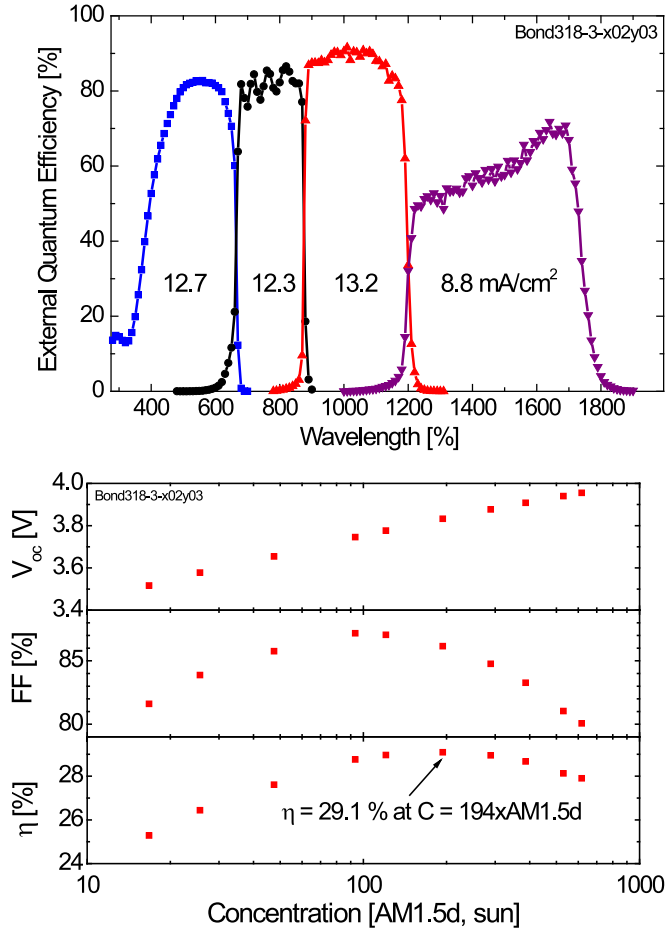

Fig. 7. External quantum efficiency of a GaInP/GaAs/GaInAs//GaSb four-junction solar cell with calculated current densities for each junction under the AM1.5d ASTMG173-3 spectrum at 1000 W/m^2 (top) and *I–V* characteristics versus concentration using the QuadFlash solar simulator (bottom), resulting in a peak efficiency of 29.1% at 194×AM1.5d.

course, this requires excellent material quality of all junctions to ensure that every absorbed photon contributes to photocurrent. However, experimental results are not far from there. We have demonstrated external quantum efficiencies above 90% and efficiencies up to 46.1% (at 312×AM1.5d) for a wafer-bonded GaInP/GaAs//GaInAsP/GaInAs solar cell grown on InP-engineered substrate. Other four-junction devices based on GaInP/GaAs//GaInAs/Ge and GaInP/GaAs/GaInAs//GaSb are still in the early development phase, but encouraging characteristics have also been obtained. This paper shows that wafer bonding is a viable method to combine III–V compound materials with significant lattice mismatch and, therefore, enables material combinations that benefit from the best possible material properties for multijunction cells.

Acknowledgment

The authors would like to acknowledge device processing and characterization by M. Piccin, N. Blanc, M. Muñoz Rico, A. Drouin, M. Scheer, K. Wagner, S. Stättner, R. Freitas, R. Koch, E. Fehrenbacher, M. Schachtner, S. K. Reichmuth, and E. Schäffer.

References

[1] W. Guter *et al.*, "III-V multijunction solar cells—New lattice-matched products and development of upright metamorphic 3J cells," in *Proc. 7th Int. Conf. Concentrating Photovoltaic Syst.*, Las Vegas, NV, USA, 2011, pp. 5–8.

[2] R. R. King *et al.*, "Solar cell generations over 40% efficiency," *Prog. Photovoltaics, Res. Appl.*, vol. 20, pp. 801–815, 2012.

[3] P. R. Sharps *et al.*, "Advances in the performance of inverted metamorphic multi-junction solar cells," in *Proc. 27th Eur. Photovoltaic Sol. Energy Conf. Exhib.*, Frankfurt, Germany, 2012, pp. 95–98.

[4] K. Sasaki *et al.*, "Development of InGaP/GaAs/InGaAs inverted triple junction concentrator solar cells," in *Proc. 9th Int. Conf. Concentrator Photovoltaic Syst.*, Miyazaki, Japan, 2013, pp. 22–25.

[5] M. A. Green *et al.*, "Solar cell efficiency tables (version 44)," *Prog. Photovoltaics, Res. Appl.*, vol. 22, pp. 701–710, Jul. 2014.

[6] S. Philipps and A. Bett, "III-V Multi-junction solar cells and concentrating photovoltaic (CPV) systems," *Adv. Opt. Technol.*, vol. 3, pp. 469–478, 2014.

[7] R. M. France *et al.*, "Quadruple-junction inverted metamorphic concentrator devices," *IEEE J. Photovoltaics*, vol. 5, no. 1, pp. 432–437, Jan. 2015.

[8] X. Sheng *et al.*, "Printing-based assembly of quadruple-junction four-terminal microscale solar cells and their use in high-efficiency modules," *Nature Mater.*, vol. 13, pp. 593–598, Apr. 28, 2014.

[9] F. Dimroth *et al.*, "Development of high efficiency wafer bonded 4-junction solar cells for concentrator photovoltaic applications," in *Proc. 40th IEEE Photovoltaic Spec. Conf.*, 2014, pp. 6–10.

[10] R. Krause *et al.*, "Wafer bonded 4-junction GaInP/GaAs//GaInAsP/GaInAs concentrator solar cells," in *Proc. AIP Conf.*, vol. 1616, 2014 pp. 45–49.

[11] P. T. Chiu *et al.*, "35.8% space and 38.8% terrestrial 5J direct bonded cells," in *Proc. IEEE 40th Photovoltaic Spec. Conf.*, 2014, pp. 11–13.

[12] F. Dimroth *et al.*, "Wafer bonded four-junction GaInP/GaAs//GaInAsP/GaInAs concentrator solar cells with 44.7% efficiency," *Prog. Photovoltaics, Res. Appl.*, vol. 22, pp. 277–282, Mar. 2014.

[13] T. N. D. Tibbits *et al.*, "New efficiency frontiers with wafer-bonded multi-junction solar cells," presented at the 29th Eur. Photovoltaic Sol. Energy Conf. Exhib., Amsterdam, Netherlands, 2014.

[14] K. Shim, H. Rabitz, and P. Dutta, "Band gap and lattice constant of $Ga_x In_{1-x} As_y Sb_{1-y}$," *J. Appl. Phys.*, vol. 88, pp. 7157–7161, 2000.

[15] E. Welser *et al.*, "Lattice-matched GaInAsSb on GaSb for TPV cells," in *Proc. 7th World Conf. Thermophotovoltaic Generation Elect.*, El Escorial, Spain, 2007, pp. 107–114.

[16] G. Létay and A. W. Bett, "EtaOpt—A program for calculating limiting efficiency and optimum bandgap structure for multi-bandgap solar cells and TPV cells," presented at the 17th Eur. Photovoltaic Sol. Energy Conf., Munich, Germany, 2001, pp. 178–181.

[17] H. A. Macleod, *Thin-Film Optical Filters*, vol. 4. London, U.K.: CRC, 2010.

[18] Ioffe Institute. Electronic archive: New Semiconductor Materials. Characteristics and Properties—Physical Properties of Semiconductors. (2015). [Online]. Available: http://www.ioffe.ru/SVA/NSM/Semicond/index.html

[19] M. Levinshtein, S. Rumyantsev, and M. Shur, Eds., *Si, Ge, C (Diamond), GaAs, GaP, GaSb, InAs, InP, InSb* (Handbook Series on Semiconductor Parameters). Singapore: World Scientific, 1996.

[20] M. Levinshtein, S. Rumyantsev, and M. Shur, Eds., *Ternary and Quaternary III-V Compounds* (Handbook Series on Semiconductor Parameters). Singapore: World Scientific, 1999.

[21] S. Adachi, "Band gaps and refractive indices of AlGaAsSb, GaInAsSb, and InPAsSb: Key properties for a variety of the 2–4 μm optoelectronic device applications," *J. Appl. Phys.*, vol. 61, pp. 4869–4876, 1987.

[22] S. Adachi, "Optical dispersion relation for GaP, GaAs, GaSb, InP, InAs, InSb, $Al_x Ga_{1-x} As$, and $In_{1-x} Ga_x As_y P_{1-y}$," *J. Appl. Phys.*, vol. 66, pp. 6030–6040, 1989.

[23] M. W. Wanlass *et al.*, "Advanced high-efficiency concentrator tandem solar cells," in *Proc. 22nd IEEE Photovoltaic Spec. Conf.*, Las Vegas, NV, USA, 1991, pp. 38–45.

[24] M. W. Wanlass *et al.*, "Practical considerations in tandem cell modeling," *Sol. Cells*, vol. 27, pp. 191–204, 1989.

[25] S. P. Philipps *et al.*, "Calibrated numerical model of a GaInP-GaAs dual-junction solar cell," *Phys. Status solidi (RRL)—Rapid Res. Lett.*, vol. 2, pp. 166–168, 2008.

[26] E. Guiot *et al.*, "Enabling InP based high efficiency CPV cells through substrate engineering and direct wafer bonding," presented at the 41st Int. Symp. Compound Semiconductors, Montpellier, France, 2014.

[27] F. Dimroth, C. Agert, and A. W. Bett, "Growth of Sb-based materials for MOVPE," *J. Crystal Growth*, vol. 248, pp. 265–73, 2003.
[28] M. Meusel, C. Baur, G. Létay *et al.*, "Spectral response measurements of monolithic GaInP/Ga(In)As/Ge triple-junction solar cells: Measurement artifacts and their explanation," *Prog. Photovoltaics, Res. Appl.*, vol. 11, pp. 499–514, 2003.
[29] G. Siefer *et al.*, "Improved grating monochromator set-up for EQE measurements of multi-junction solar cells," in *Proc. 39th IEEE Photovoltaic Spec. Conf.*, Tampa, FL, USA, 2013, pp. 86–89.
[30] M. Meusel *et al.*, "Spectral mismatch correction and spectrometric characterization of monolithic III-V multi-junction solar cells," *Prog. Photovoltaics, Res. Appl.*, vol. 10, pp. 243–255, 2002.
[31] G. Siefer *et al.*, "Influence of the simulator spectrum on the calibration of multi-junction solar cells under concentration," in *Proc. 29th IEEE Photovoltaic Spec. Conf.*, New Orleans, LA, USA, 2002, pp. 836–839.
[32] M. Schachtner *et al.*, "Analysis of a four lamp flash system for calibrating multi junction solar cells under concentrated light," presented at the 11th Int. Conf. Concentrater Photovoltaic Syst., Chambery, France, 2015.
[33] S. Essig and F. Dimroth, "Fast atom beam activated wafer bonds between n-Si and n-GaAs with low resistance," *ECS J. Solid State Sci. Technol.*, vol. 2, pp. Q178–Q181, 2013.
[34] S. Essig *et al.*, "Fast atom beam-activated n-Si/n-GaAs wafer bonding with high interfacial transparency and electrical conductivity," *J. Appl. Phys.*, vol. 113, pp. 203512-1–203512-6, May 28, 2013.
[35] D. Häussler *et al.*, "Aberration-corrected transmission electron microscopy analyses of GaAs/Si interfaces in wafer-bonded multi-junction solar cells," *Ultramicroscopy*, vol. 143, pp. 55–61, 2013.

Authors' photographs and biographies not available at the time of publication.